Defect Structure of $(B_2O_3)_{100-x}$ $(Bi_2O_3)_x$ glasses

M. Mohsen[*], E. Gomaa[*], M.Sh. Al-Kotb[*], M. Abdel-Baki[+], and N. Fathy[**]

[*]*Phys. Dept. Faculty of Science, Ain Shams University, Cairo, Egypt.*
[+] *National Research Center, Glass Department, Dokki, Giza, Egypt.*
[**] *Phys. Dept. Faculty of Engineering, Modern Academy, Cairo, Egypt.*

Bismuth borate glasses with composition $(100-x)B_2O_3 - x (Bi_2O_3)$ (where x is in mol.% ranging from 25 -50 in steps of 5) have been prepared by using melt quenching technique. Positron annihilation lifetime (PAL), Fourier transform infra-red (FT-IR) and X-ray diffraction (XRD) measurements have been performed to study the amorphous and defect structure as well as the vibrating band structure. PAL results have revealed weak formation of ortho-positronium (o-Ps) at amorphous sites. At low concentration, the pore size at these sites increases from 2.5 nm to 3.5 nm with increase of Bi_2O_3 content, then show weak decrease to 3nm at higher concentration showing also a reduction in the relative pore fraction from 9.8% to 1% in agreement with XRD spectra, which indicate the presence of some peaks associated with Bi_2O_3 phase. On the other hand, the variation of the annihilation parameters at defects, suggest strong trapping of the free positron at non-bridging oxygen (NBO) bonds, which have been determined by FT-IR. In addition, IR spectra revealed the presence of some bonds that are assigned to vibrations of Bi-O bonds from $[BiO_3]$ pyramidal and $[BiO_6]$ octahedral units and B-O bonds from $[BO_3]$ and $[BO_4]$ units.

1. Introduction

Glasses based on bismuth oxide Bi_2O_3 have wide applications in the field of opto-electronic devices, thermal and mechanical sensors as well as reflecting windows [1, 2].

The IR physical properties are characterized by high refractive index, excellent infrared transmissions, high non linear optical susceptibility, as well as high polarizability [3, 4]. In these glasses the bismuth ions may appear as BiO_3 pyramidal or BiO_6 octahedral units [4, 5].

Bi_2O_3 cannot be considered as network former due the small field strength of Bi^{3+} ion [6]. However in combination with B_2O_3, glass formation is possible in a relatively large compositional range [7]. B_2O_3 is one of the most common glasses former. According to Krogh-Moe [5], the structure of vitreous B_2O_3 consists of a random network of boroxyl rings and BO_3 triangles connected by B-O-B linkages. Moreover, the addition of modifier such as heavy metal oxide in borate glasses could produce the conversion of the triangular BO_3 structural units to BO_4 tetrahedral with a coordination number four [8].

Among these borates, it has been shown, that the monoclinic bismuth borate $Bi_2B_3O_6$ has remarkably large linear and nonlinear optical coefficients [9]. Calculations indicate that this can be mainly due to the contribution of the $[BiO_4]^{5-}$ anionic group [10]. Enhancement in the linear and nonlinear optical properties in oxide glasses is due to the generation of non bridging oxygen (NBO) bonds, which are known to have a high electron density than the bridging oxygen[11,12]. In addition, they lead to loosening of the structure and increase of disorder short range. Their relative abundance is important in determining [13] the optical thermodynamic and dynamic properties of glasses.

In the present work, positron annihilation lifetime (PAL), X-ray diffraction (XRD), and Fourier Transform Infrared-Red (FT-IR) are performed to determine the effect of increasing bismuth oxide content in the glass system Bi_2O_3-B_2O_3 on the amorphous and vibrational structures as well as the relative abundance of NBO bonds.

2. Experimental

2.1. Glass preparation

Bismuth borate glasses of compositions $(B_2O_3)_{(100-x)}$ $(Bi_2O_3)_x$ (x in mol% and ranging from 25 to 50 in steps of 5 mol %) have been prepared by melt quenching method. The stoichiometric powders of H_3BO_3, and Bi_2O_3 with 99.99% high purity (AR purity) are thoroughly mixed and loaded into porcelain crucibles. The melts are thoroughly homogenized at the temperature range of 700-1000°C for 2 hours. The melt is then stirred occasionally for proper mixing. After the disappearance of the bubbles, the melt is poured and loaded into two stainless steel plates maintained at 200°C. The glasses thus obtained are found to be transparent and yellowish in color. In order to recognize the composition easily, the glass samples are named orderly as BB1, BB2, BB3, BB4, BB5, BB6 for x=25, 30, 35, 40, 45, and 50 mol.% of Bi_2O_3 respectively. The samples with higher Bi_2O_3 content is not considered due to the occurrence of spontaneous crystallization.

2.2. Measurements

2.2.1. The FT-IR Spectroscopy

The infrared (IR) spectra of the glasses were recorded at room temperature in the range 400-4000 cm^{-1} using FTIR spectrometer. The samples are crushed in an agate mortar in order to obtain particles of micrometer size. This procedure is applied every time to fragments of bulk glass to avoid structural modifications due to ambient moisture.

2.2.2. The X-ray Diffraction (XRD)

Powder X-ray diffraction (XRD) spectra for all the glass samples in the present investigation are recorded at room temperature using a PW 1830 diffractometer with Cu Kα radiation (40 KV x 25 mA) and a graphite monocromator with 2θ (θ being Bragg angle) from 10° to 90°.

2.2.3. Positron Annihilation lifetime spectroscopy

PAL measurements have been performed using a conventional fast-fast coincidence system. About 20 μCi of ^{22}Na positron source is used. The time resolution of the system (Full-Width at Half-Maximum, FWHM) was 240 ps for ^{60}Co with a time calibration 25 ps/ch. In PAL spectrum about 1.5 million counts were accumulated. The numerical analysis of PAL spectra were performed by PATFIT [14] and LT 9.0 [15] using three Gaussian resolution functions and resolved into three lifetime components without source correction, the variance of fit was less than 1.2.

In amorphous materials a fraction of the positrons will capture an electron and form a bound state, which is called postronium (Ps) and can be in two spin states [para-postronium (p-Ps) and ortho-postronium (o-Ps)].

Also, the lifetime spectra were analyzed into three components using the PATFIT program. The component characterized by lifetime τ_1 and intensity I_1 represents positron annihilating in monovacancies and dislocation loops. The components with τ_2 and I_2 characterize positrons trapped and annihilating in three-dimensional vacancies. The component characterized by lifetime τ_3 and intensity I_3 directly correlates with the size of pores in the amorphous regions by using the Tao- Eldrup semi-empirical [16, 17]. The cavity hosting Ps is assumed to be a spherical void with effective radius R. The relationship between τ_3 and radius R is given as follows:

$$t_3 = 0.5 \left[\frac{\Delta R}{R + \Delta R} + \frac{1}{2p} \sin \left(2p \frac{R}{R + \Delta R} \right) \right]^{-1} \quad (1)$$

where the units of R and τ_3 are $\overset{o}{A}$ and ns, respectively and $\Delta R = 1.656 \ \overset{o}{A}$ for amorphous materials and is derived from fitting the observed o-Ps lifetimes in molecular solids with known hole sizes [18]. Furthermore, the pore fraction F is evaluated in terms of the o-Ps intensity I_3 (which is proportional to the probability of formation of o-Ps and the volume pore ($V = 4\pi R^3 /3$) by the equation:

$$F = CV \ I_3 \tag{2}$$

where C is a constant. Usually, we use relative fraction F_r

$$F_r = \frac{F}{C} = VI_3 \tag{3}$$

3. Results and Discussions

3.1. The X-ray Diffraction Pattern

All the glass samples are shown in Fig.(1) which confirms the amorphous nature of the prepared samples at low concentration of Bi_2O_3 due to the absence of Bragg peaks. At higher concentration some peaks appear in the spectra indicating a certain phase of Bi_2O_3.
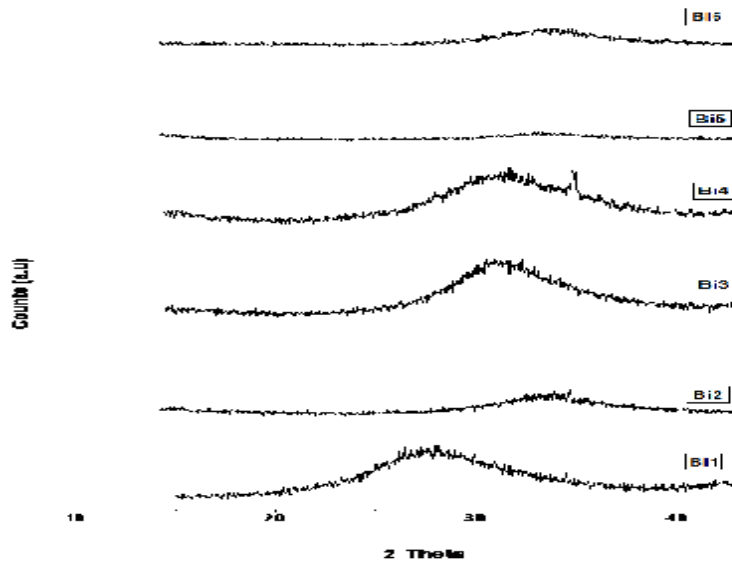

Fig.(1): X-Ray diffraction patterns for studied glasses, Bi_2O_3 content increases from bottom to top**.**

3.2. The infrared absorption spectrum

The FT-IR spectra of bismuth borate glass samples with different Bi_2O_3 concentration shows the absorption as a function of wavenumber Fig.(2).
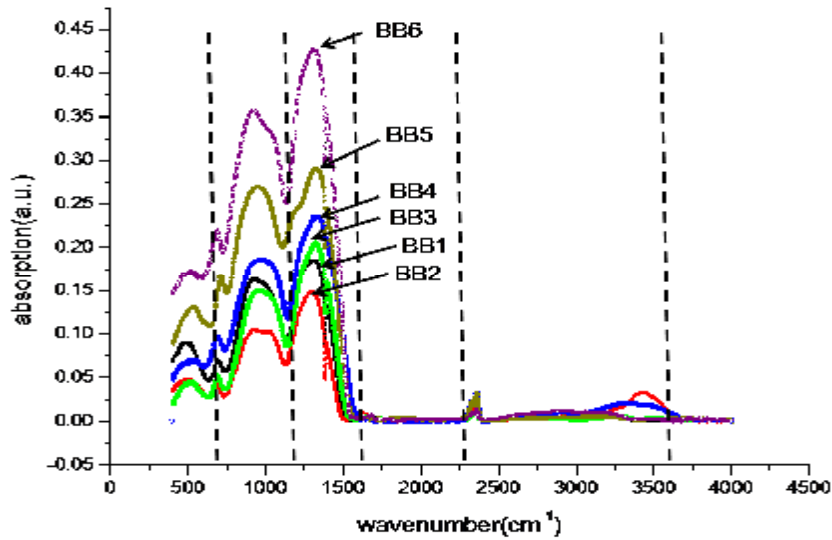

Fig.(2):FT-IR spectra of studied glasses

The infrared spectrum has shown medium, weak, and broad absorption bands. Hence the effect of composition on various types of structural units within each series is not much significant. The finger print infrared absorption peaks of active borate network vibrational modes are present in all the series of glasses. The absorption peaks in FTIR spectra can be divided into four main groups in the ranges 3600-2300 cm^{-1}, 1600-1200 cm^{-1}, 800-1200 cm^{-1}, 700-400 cm^{-1} (see Fig. 2).

The weak band observed at ~1650-1690 cm^{-1} is due to OH bending mode of vibration [19]. The origin of this weak band may be due to the trapping of water molecules in the glass matrix during the decomposition of boric acid. The broad and strong band observed in the range ~1310-1340 cm^{-1} is due to γ_3 mode of planar BO_3 group whereas the broad and strong band at ~ 1020-1030 cm^{-1} is due to γ_1 mode of BO_4 tetrahedral. These bands become more intense with increase of Bi_2O_3 content except for BB2. The shoulder around 1234 cm^{-1} found in this glass system is assigned to the B-O stretching vibrations of $(BO)^{-3}$ units with non-bridging oxygen atoms [19, 20].this result indicates that the number of non- bridging oxygen atoms increases with increase the content of Bi_2O_3.

The peaks around 840 cm^{-1} becomes more predominant as the Bi$_2$O$_3$ content increases and is related to the symmetrical stretching vibration of the Bi-O bonds in the [BiO$_3$] groups [21]. The strong band at~700 cm^{-1} is due to the bending vibration of B-O-B linkages of BO$_3$ units [22, 23]. The weak band observed at ~520 cm^{-1} is due to γ_4 vibrations of BO$_4$ tetrahedral and the weak bands below 500 cm^{-1} are due to Bi-O vibrations [24, 25].

The increase in Bi$_2$O$_3$ content in the present glass system transforms the structure into a bismuthate one formed by [BiO$_6$] and [BiO$_3$] groups. The band positions and the corresponding assignments are given in table (2) for all the glass compositions.

Table (2): Band positions and corresponding assignments of IR spectra of all glass compositions

Bands	Assignment
420-500 cm^{-1}	Bi-O- Bi vibration in [BiO$_6$] octahedral units [8]
510-610 cm^{-1}	[BO$_4$] tetrahedral [25,29]
680-720 cm^{-1}	Bending vibrations of B-O-B in [BO$_3$] triangles [27,28]
900-950 cm^{-1}	Stretching vibrations of B-O bonds in [BO$_4$] from diaborate groups[25]
1020 -1080 cm^{-1}	γ_1 mode of BO$_4$ tetrahedral stretching vibrations[29]
1230-1240 cm^{-1} (shoulder at 1234 cm^{-1})	B-O stretching vibrations of [BO]$^{-3}$ units with non-bridging oxygen atoms [26,27]
1310-1400 cm^{-1}	stretching vibrations of B-O-B in [BO$_3$] triangles[19-27]
1630-1690 cm^{-1}	OH bending mode of vibration [28]
1700-3000 cm^{-1}	[H-O-H] [28]

~715, 840,880 symmetrical stretching vibration of the Bi-O bonds in the [BiO$_3$] groups. [8, 23, 28].

~990 stretching vibrations of B-Φ bonds in B Φ_4 units from tri-, tetra-, and penta- borate groups. [28].

~1295 asymmetrical stretching vibrations of B-O bonds in BO$_3$ and B Φ_2O- units. [28].
{Where Φ is an oxygen atom bridging two boron atoms}.

3.3. Positron Annihilation Spectra:

Figure (3 and 4), show the lifetime τ_3 and intensity I_3 describing the annihilation parameters of the o-Ps in amorphous regions. With increasing Bi_2O_3 content, τ_3 increases from 1.5 ns to 2.9 ns at low concentrations then decreases to an average of 2.2 ns at higher concentration by using equation(1), this corresponds to a change in the pore size at the amorphous region from 2.5 nm to 3.5 nm (Fig.3).

However I_3 indicates a weak average formation probability for o-Ps, which increases to reach 2 % at Bi_2O_3 content of 40 % then decreases at higher concentrations (Fig.4).
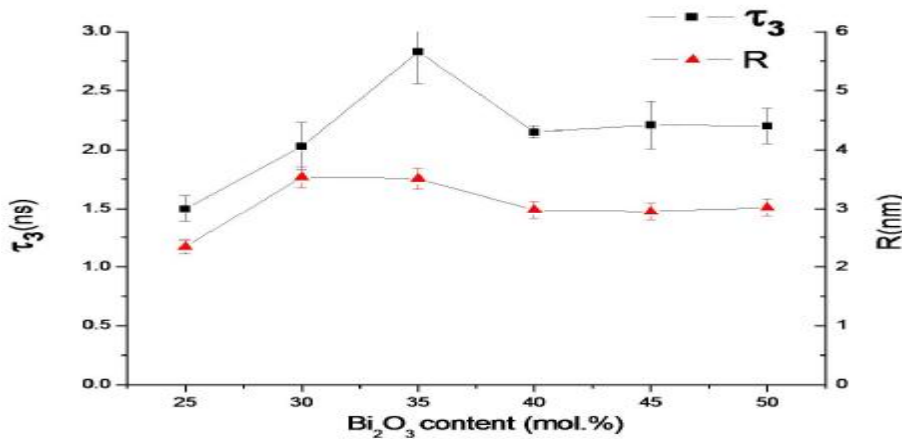

Fig.(3): Relation between the radius (R)(nm) and lifetime (τ_3)(ns) as a function of Bi_2O_3 content (The line drawn is only for guiding the eye)
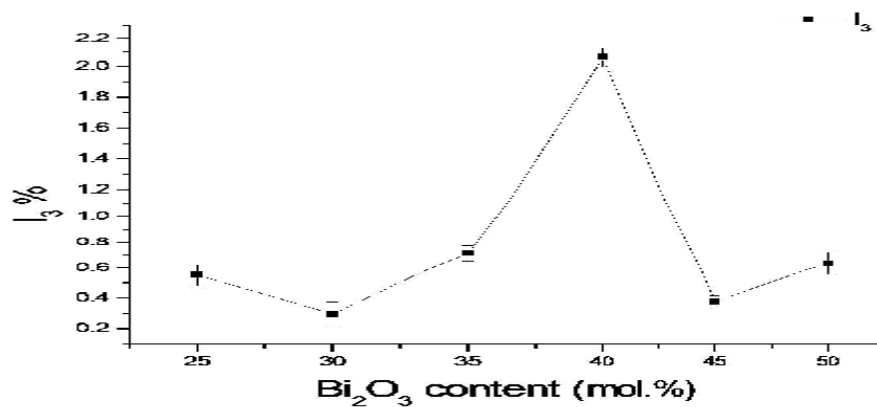

Fig. (4): Variation of intensity I_3(%) with Bi_2O_3 content (The line drawn is only for guiding the eye)

Figure (5), represents the variation of the relative pore fraction with Bi_2O_3 concentration as calculated from eqn.(3) which shows a decrease from 9.8% to 1%.
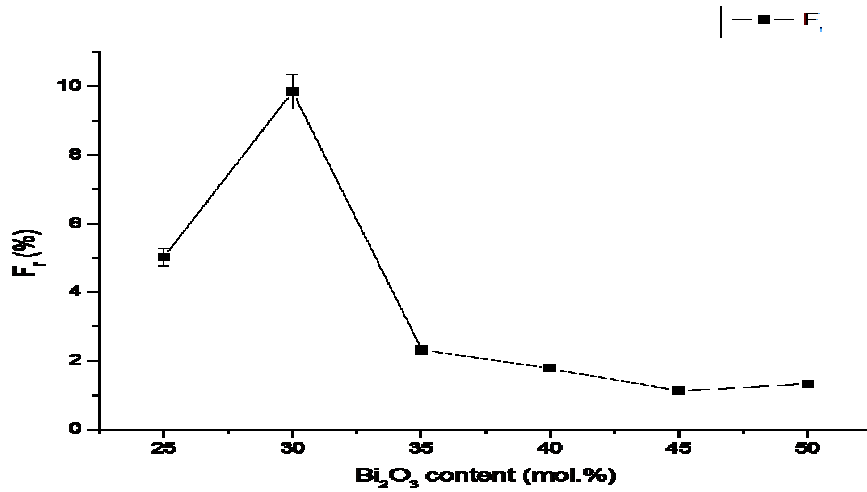

Fig. (5): Variation of relative pore fractions F_r(%) with Bi_2O_3 content (The line drawn is only for guiding the eye)

Fig. (6) and (7) show the lifetime τ_2 and intensity I_2, for the annihilation of free positrons with electrons in open volume defects. τ_2 increases first with increasing Bi_2O_3 content, then decreases showing weak variation at large Bi_2O_3 content. The reduction in τ_2 can be explained by an enhancement in the electron density.
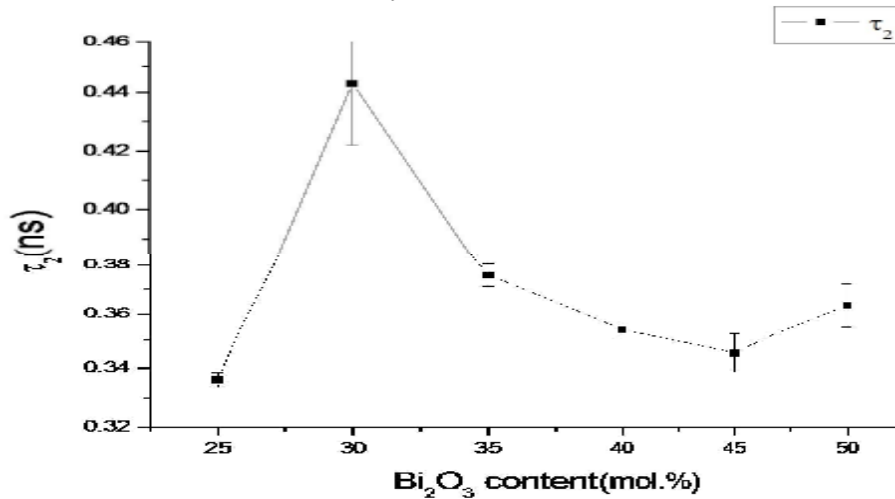

Fig. (6): Variation of τ_2 (ns) with Bi_2O_3 content (The line drawn is only for guiding the eye)
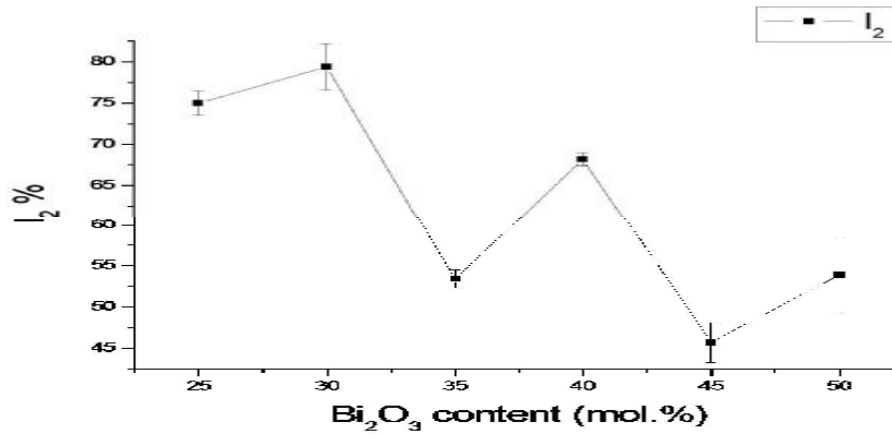
Fig.(7): Variation of I_2 (%) with Bi_2O_3 content (The line drawn is only for guiding the eye)

The percentage of population of these sites reaches 79% at low Bi_2O_3 content then decreases to an average of 55% at higher Bi_2O_3 content indicating that the annihilation in the Bi_2O_3-B_2O_3 glass system occurs mainly either as free annihilation or self annihilation of p-Ps (see fig.8).
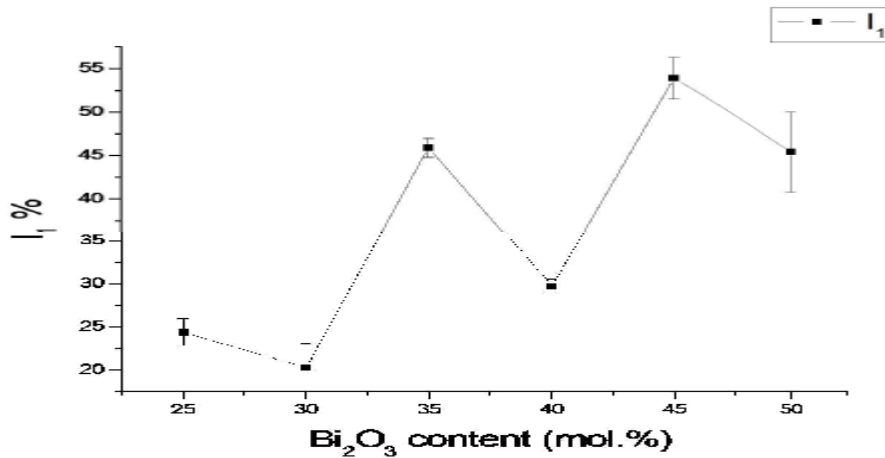

Fig. (8): Variation of I_1 (%) with Bi_2O_3 content (The line drawn is only for guiding the eye)

From the FT-IR measurements, the shoulder around 1234 cm^{-1} has been assigned to the B-O stretching vibrations of $(BO)^{-3}$ units with non-bridging oxygen atoms (NBO). Applying the IR deconvolution of the spectra at different Bi_2O_3 composition, the area under the shoulder around

1234cm^{-1} has been deduced, which is a measure of the number of NBO atoms Fig. (9). At low Bi_2O_3 content (25-35%) the number decreases, which constitutes an explanation for the decrease in the population percentage of positrons I_2 to 52% Fig.(7) as well as the increase in τ_2. At higher Bi_2O_3 content the number of NBO atoms increases, which is associated with an increase in I_2 to 67% due to an enhancement in the electron density. This explains also the reduction in τ_2 from 0.44 ns to an average of 0.36 ns.
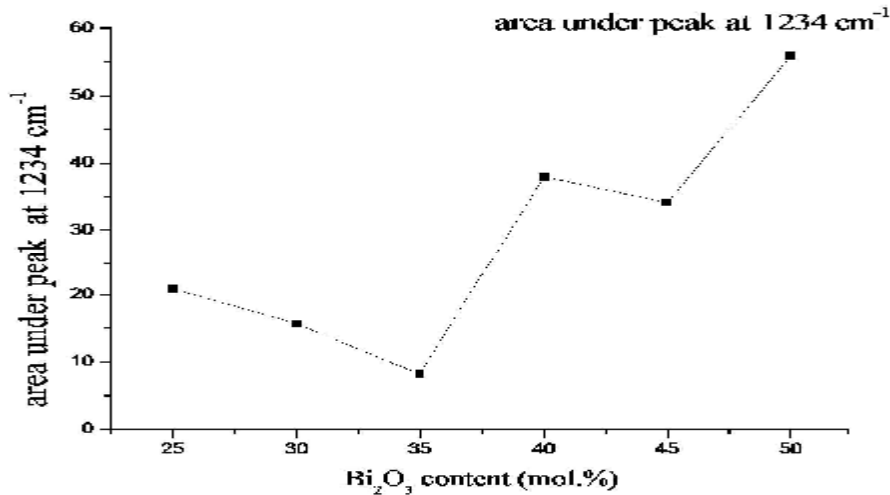

Fig. (9): Variation of the area under the peak at 1234 cm^{-1} with the Bi_2O_3 content
(The line drawn is only for guiding the eye)

4. Conclusion:

1- XRD results a reduction in the amorphous nature with increasing Bi_2O_3 concentration when, some peaks appear as a certain phase of Bi_2O_3. Also, ortho-positronium (o-Ps) trapping in amorphous sites revealed the decrease of pore size and fraction with Bi_2O_3 content.

2- The increase in Bi_2O_3 content in this glass system transforms the structure into a bismuthate one formed by $[BiO_6]$ and $[BiO_3]$ groups.

3- FT-IR measurements have identified, among others, the B-O stretching vibrations of (BO)$^{-3}$ units with NBO atoms, which are found to increase with Bi_2O_3 content, in agreement with the reduction of the lifetime of free positrons from 440 ps to 360 ps due to the resulting increase of electron density at these damping bonds.

4- Positron annihilation lifetime technique has proven successful to study amorphous structure and NBO atoms in glass systems.

5. Acknowledgement:

References:

1. D.W. Hall, M.A. Newhouse, N.F. Borelli, W.H. Dumbaugh and D. L. Weidman, *Appl. Phys. Lett*. **54**, 1293 (1989).

2. C. Stehle, C. Vira, D. Hogan, S. Feller and M. Affatigato, *Phys. Chem. Glasses*, **39 (2)**, 83 (1998).

3. (a) J. Lorosch, M. Couzi, J. Pelovz, R. Vacher, and A. Lavascur, *J. Non –cryst. Solids*, **69**, 1 (1984);
   (b) A.C. Wright, N.M. Vedischeheva and B.A. Shakhmatahim, *J. Non-cryst. Solids*, **192**, 92 (1995).

4. W.H. Dumbaugh and J.C. Lapp, *J. Am. Ceram. Soc*., **75**, 2315 (1992).

5. J. Krogh-Moe, *Phys. Chem. Glasses*, **3**, 101 (1962).

6. G. El-Damrawi and K. El-Egili, *Physica*, B **299**, (2001).

7. K. Gerth and C. Russel, *J. Non-Cryst. Solids*, **221**, 10 (1997).

8. Y. Dimitriev and V.T. Mihailova, *J. Sci. Lett*., **9**, 1251 (1990).

9. H. Hellwing, J. Liebertz and L. Bohaty, *J. Appl. Phys*., **88**, 240 (2000).

10. Z. Lin, Z. Wang, C. Chen and M. H. Lee, *J. Appl. Phys*., **90**, (2001).

11. M. Abdel-Baki, F. El-Diasty and F. Abdel Wahab, *Opt. Comm*, **261**, 65 (2006).

12. N. Jiang, *Solid State Comm*., **122**, 7 (2002).

13. N. Jiang, J. Qiu and J. Silcox, *J. Appl. Phys*., Lett.**77**, (2000).

14. PATFIT Pakage, Riso National Laboratory, Denmark, (1989).

15. A. Dupasquier and A.P. Mills, Jr., ed.: *Positron Spectroscopy of Solids*, IOS Press, Amsterdam, The Netherlands, (1995).

16. S. J. Tao, *J. Chem. Phys*., **56(12)**, (1972).

17. M. Eldrup, D. Lightbody and N. Sherwood, *J. Chem. Phys*., **63**, (1981).

18. H. Nakanishi, S. J. Wang, and Y. C. Jeans,"*Microscopic Surface Tension Studied by Positron Annihilation*." Positron Annihilation Studies of Fluids, Sharma, S. c., Ed.; World Sci. Pub. : Singapore, (1988).

19. B.V.R. Chowdrai and Z. Rong, *Solid State Ionics*, **90**, (1996).

20. Shashidhar Bale, N. Srinivas Rao and Syed Rahaman, *Solid State Sci*., **10**, 326 (2008).

21. S. Hazra and A. Ghosh, *Phys. Rev*., B **51**, 851 (1995).

22. G. Sharma, K. Singh, Manupriya, S. Mohan, H. Singh and S. Bindra, *Radiat. Phys. Chem*., **75 (9)**, (2006).

23. E. R. Shaaban, M. Shapaan and Y.B. Saddeek, *J. Phys.: Conden. Matter*, **20**, 155 (2008).

24. R. Iordanova, V. Dimitrov, Y. Dimitriev and D. Klissurski, *J. Non-Cryst. Solids*, **180**, (1994).

25. B. Karthikeyan and S. Mohan, *Physica*, B **334**, 300 (2003).

26. K. Singh, *Solid State Ionics*, **93**, 147 (1997).

27. E.I. Kamitsos, A.P. Patsis, M.A. Karakassides and G.D. Chryssikos, *J. Non-Cryst. Solids*, **126**, (1990).

28. A.K. Hassan, L. Borjesson and L.M. Torell, *J. Non-Cryst. Solids*, **172–174**, (1994).

29. L. Baia, R. Stefan, J. Popp, S. Simon and W. Kiefer, *J. Non-Cryst. Solids*, **324**, (2003).